Monte Carlo simulation study of a selforganisation process leading to ordered precipitate structures

F. Zirkelbach [a,*] M. Häberlen [a] J. K. N. Lindner [a] B. Stritzker [a]

[a] *Universität Augsburg, Institut für Physik, Universitätsstrasse 1, D-86135 Augsburg, Germany*

Abstract

Periodically arranged, selforganised, nanometric, amorphous precipitates have been observed after high-fluence ion implantations into solids for a number of ion/target combinations at certain implantation conditions. A model describing the ordering process based on compressive stress exerted by the amorphous inclusions as a result of the density change upon amorphisation is introduced. A Monte Carlo simulation code, which focuses on high-fluence carbon implantations into silicon, is able to reproduce experimentally observed nanolamella distributions as well as the formation of continuous amorphous layers. By means of simulation, the selforganisation process becomes traceable and detailed information about the compositional and structural state during the ordering process is obtained. Based on simulation results, a recipe is proposed for producing broad distributions of ordered lamellar structures.

Key words: Monte Carlo simulation; Selforganisation; Precipitation; Amorphisation; Nanostructures; Ion irradiation

PACS: 02.70.Uu; 61.72.Tt; 81.16.Rf

* Corresponding author.

Tel.: +49-821-5983008; fax: +49-821-5983425.

1 Introduction

Precipitates resulting from high-fluence ion implantation into solids are usually statistically arranged and demonstrate a wide size distribution. However, the formation of ordered lamellar inclusions has been observed for a number of ion/target combinations at certain implantation conditions [1-3]. An inevitable condition for the material to exhibit this unusual selforganised arrangement is a largely reduced density of host atoms in the amorphous phase compared to the crystalline host lattice. As a consequence stress is exerted by the amorphous inclusions, which is responsible for the ordering process. A model describing the process is implemented in a simulation code, focussing on high-fluence carbon implantations into silicon. Simulation results are compared to experimental data and a recipe for the fabrication of broad distributions of ordered lamellar structures is proposed.

2 Model

High-fluence carbon implantations in silicon at temperatures between 150 and 400 °C with an energy of 180 keV result in an amorphous buried SiC_x layer along with ordered spherical and lamellar amorphous SiC_x inclusions at the upper layer interface [4] (Fig. 1). A model [5] explaining the evolution of ordered lamellae with increasing amounts of implanted carbon is shown schematically in Fig. 2.

With increasing fluence the silicon becomes supersaturated with carbon atoms, resulting in the nucleation of spherical SiC_x precipitates. By the precipitation into the amorphous SiC_x (a-SiC_x) phase an enormous interfacial energy can be saved, which would be required for cubic SiC ($3C - SiC$) in crystalline silicon (c-Si) [6], originating from a 20 % lattice mismatch. Since amorphous silicon (a-Si) is not stable against ion beam induced epitaxial recrystallisation

E-mail address: frank.zirkelbach@physik.uni-augsburg.de (Frank Zirkelbach)

at temperatures above 130 °C at the present low atomic displacement rates [7], the existence of the amorphous precipitates must be due to the accumulation of carbon (carbon induced amorphisation), which stabilises the amorphous phase [8]. In fact, energy filtered XTEM studies [9] reveal the carbon-rich nature of the precipitates.

The Si atomic density of a-SiC is about 20 to 30 % lower than that of $3C-SiC$ [10,11]. Thus a corresponding density reduction is also assumed for substoichiometric a-SiC_x compared to c-Si. Therefore the amorphous volumes tend to expand and as a result compressive stress is exerted on the Si host lattice, represented by black arrows in Fig 2. This stress may relax in the vertical direction since the process occurs near the target surface. Upon continued ion irradiation, regions between amorphous inclusions are more likely to turn into an amorphous state as the stress disturbs the rearrangement of atoms on regular lattice sites (stress enhanced amorphisation). In contrast, randomly formed amorphous precipitates (ballistic amorphisation) with low concentrations of carbon in a crystalline neighbourhood are likely to recrystallise under present implantation conditions.

Since the solid solubility of carbon in c-Si is essentially zero, once formed, a-SiC_x inclusions serve as diffusional sinks for excess carbon atoms in the c-Si phase, as represented by the white arrows in Fig. 2. As a consequence the amorphous volumes accumulate carbon, which stabilises them against recrystallisation and promotes the strain supported formation of additional a-SiC_x in their lateral vicinity.

3 Simulation

For the Monte Carlo simulation the target is divided into cells with a cube length of 3 nm. Each cell is either in a crystalline or an amorphous state and stores the local carbon concentration. The simulation starts with a complete crystalline target and zero carbon concentration.

The simulation algorithm consists of three parts. In a first amorphisation/recrystallisation step random numbers are computed to specify the volume at position $\vec{r}$ in which a collision occurs. Two uniformly distributed random numbers x and y are generated to determine the lateral position of $\vec{r}$. Using the rejection method, a random number z specifying the depth coordinate of $\vec{r}$ is distributed according to the nuclear stopping power profile which, as will be seen below, is identical to the number of collisions caused by the ions per depth. The local amorphisation or recrystallisation probability is computed as detailed below and another random number between 0 and 1 determines whether there is amorphisation or recrystallisation or the state of that volume is unchanged. This step is repeated for the mean number of steps of cells in which collisions are caused by one ion, gained from *TRIM* [12] collision data. In a second step, the ion is incorporated in the target at randomly chosen coordinates with the depth coordinate being distributed according to the *TRIM* implantation profile. In a last step, the carbon diffusion, controlled by two simulation parameters d_v and d_r, as well as sputtering, controlled by the parameter n are treated. For every d_v simulation steps, a fraction d_r of the amount of carbon in crystalline volumes is transfered to an amorphous neighbour in order to allow for a reduction of the supersaturation of carbon in crystalline volumes. For every n steps, a crystalline, carbon-free layer is inserted at the bottom of the cell array while the first layer is removed, where n results from a RBS derived [5] sputter rate.

In order to calculate the amorphisation probability, three factors have to be taken into account corresponding to our model. In the simulation, each of these mechanisms contributes to a local amorphisation probability of the cell at $\vec{r}$. The strength of each mechanism is controlled by simulation parameters. The local amorphisation probability at volume $\vec{r}$ is calculated by

$$p_{c\to a}(\vec{r}) = p_b + p_c c_C(\vec{r}) + \sum_{\text{amorphous neighbours}} \frac{p_s c_C(\vec{r'})}{(r-r')^2} \ . \qquad (1)$$

The normal (ballistic) amorphisation is controlled by p_b and is set to constant.

This choice is justified by analysing *TRIM* collision data that show identical depth profiles for the number of collisions per depth and the nuclear stopping power. Thus, on average an ion loses a constant amount of energy per collision. The carbon induced amorphisation is proportional to the local amount of carbon $c_C(\vec{r})$ and controlled by weight factor p_c. The stress enhanced amorphisation is weighted by p_s. The forces originating from the amorphous volumes $\vec{r'}$ in the vicinity of $\vec{r}$ are assumed to be proportional to the amount of carbon $c_C(\vec{r'})$ in the neighbour cell. The sum is limited to volumes located in the same layer because of stress relaxation towards the surface. Since the stress amplitude decreases with the square of the distance $r - r'$, a cutoff radius is used in the simulation. If an amorphous volume is hit by collisions, a recrystallisation probability is given by

$$p_{a\to c}(\vec{r}) = (1 - p_{c\to a}(\vec{r}))\left(1 - \frac{\sum_{direct\,neighbours}\delta(\vec{r'})}{6}\right), \tag{2}$$

$$\delta(\vec{r}) = \begin{cases} 1 \text{ if the cell at position } \vec{r} \text{ is amorphous} \\ 0 \text{ otherwise} \end{cases}$$

which is basically 1 minus the amorphisation probability and a term taking into account the crystalline neighbourhood which is needed for epitaxial recrystallisation.

4 Results

First versions of this simulation covered only the limited depth region of the target in which selforganisation is observed [13,14]. As can be seen in Fig. 3, the new version of the simulation code is able to model the whole depth region affected by the irradiation process and properly describes the fluence dependence of the amorphous phase formation. In Fig 3a) only isolated amorphous cells exist in the simulation and cross-section transmission electron microscopy (XTEM) shows dark contrasts, corresponding to highly distorted regions caused by defects. XTEM at higher magnification [9] shows the exis-

tence of amorphous inclusions of $3\,nm$ in size. For a fluence of $2.1 \times 10^{17} cm^{-2}$ a continuous amorphous layer is formed (Fig. 3b). The simulation shows a broader continuous layer than observed experimentally. However, dark contrasts below the continuous layer in the XTEM image of Fig. 3b) indicate a high concentration of defects and amorphous inclusions in this depth zone. The continuous amorphous layer together with the region showing the dark contrast has essentially the same thickness as the simulated continuous layer. For higher fluences (Fig. 3c and d) experimental and simulated data correspond to a high degree. The thickness of the continuous amorphous layer increases with increasing fluence. Next to the upper crystalline/amorphous interface, nanometric lamellar inclusions are formed which become more defined with increasing fluence, reflecting the progress of selforganisation. The difference in depth throughout all images is due to a deeper maximum of the used *SRIM* implantation profile compared to older, more accurate *TRIM* versions.

By the simulation it is possible to determine the carbon concentration in crystalline and amorphous volumes. This is shown in Fig. 4. Lamellae exist between 350 and $400\,nm$ and cause a fluctuation in the carbon concentration. This is due to the carbon diffusion, which is of great importance for the ordering process, as already pointed out in [13,14], and the complementarily arranged and alternating sequence of layers with high and low amounts of amorphous regions. In addition, a saturation limit of carbon in c-Si under the given implantation conditions can be identified between 8 and $10\,at.\%$, the maxima of carbon concentration in crystalline volumes.

Based on the above results, a recipe is proposed to create thick layers with a lamellar structure that might be suitable for applications. The starting point is a crystalline silcon target with a nearly constant carbon concentration of $10\,at.\%$ in a $500\,nm$ thick surface layer. This can possibly be achieved by multiple energy (180 to $10\,keV$) carbon implantation at a temperature of $500\,^{\circ}$C, preventing amorphisation [5]. In a second step the target is irradiated at $150\,^{\circ}$C with $2\,MeV\ C^{+}$ ions, which have a nearly constant energy loss in the top $500\,nm$ and do not significantly change the carbon concentration

here. The result is displayed in Fig. 5. Ordered structures already appear after 100×10^6 steps corresponding to a fluence of $D = 2.7 \times 10^{17} cm^{-2}$ and become more defined with increasing fluence. According to recent studies [15] these structures are expected to be the starting point for materials showing strong photoluminescence.

5 Summary and conclusion

Ion irradiation of solids at certain implantation conditions may result in the formation of regularly ordered amorphous precipitates. The ordering process can be understood by means of the model presented here, which is able to reproduce experimental observations after translation into a Monte Carlo simulation code. Detailed information have been collected, such as the amount of carbon in amorphous and crystalline volumes, shedding light on the selforganisation process. The MC simulation even predicts correctly the depth position of continuous amorphous layers. Finally a technique is proposed to produce thick films of ordered lamellar nanostructures.

References

[1] A. H. van Ommen, Nucl. Instr. and Meth. B 39 (1989) 194.

[2] E. D. Specht, D. A. Walko, S. J. Zinkle, Nucl. Instr. and Meth. B 84 (1994) 323.

[3] M. Ishimaru, R. M. Dickerson, K. E. Sickafus, Nucl. Instr. and Meth. B 166-167 (2000) 390.

[4] J. K. N. Lindner, M. Häberlen, M. Schmidt, W. Attenberger, B. Stritzker, Nucl. Instr. Meth. B 186 (2002) 206.

[5] J. K. N. Lindner, Nucl. Instr. Meth. B 178 (2001) 44.

[6] W. J. Taylor, T. Y. Tan, U. Gösele, Appl. Phys. Lett. 62 (1993) 3336.

[7] J. Linnross, R. G. Elliman, W. L. Brown, J. Matter. Res. 3 (1988) 1208.

[8] E. F. Kennedy, L. Csepregi, J. W. Mayer, J. Appl. Phys. 48 (1977) 4241.

[9] M. Häberlen, Bildung und Ausheilverhalten nanometrischer amorpher Einschlüsse in Kohlenstoff-implantierten Silizium, Diploma thesis, Augsburg, 2002 (in Germany).

[10] L. L. Horton, J. Bentley, L. Romana, A. Perez, C. J. McHargue, J. C. McCallum, Nucl. Instr. Meth. B 65 (1992) 345.

[11] W. Skorupa, V. Heera, Y. Pacaud, H. Weishart, in: F. Priolo, J. K. N. Lindner, A. Nylandsted Larsen, J. M. Poate (Eds.), New Trends in Ion Beam Processing of Materials, Eur. Mater. Res. Soc. Symp. Proc. 65, Part 1, Elsevier,Amsterdam, 1997,p. 114.

[12] J. F. Ziegler, J. P. Biersack, U. Littmark, The Stopping and Range of Ions in Solids, Pergamon, New York, 1985.

[13] F. Zirkelbach, M. Häberlen, J. K. N. Lindner, B. Stritzker, Comp. Matter. Sci. 33 (2005) 310.

[14] F. Zirkelbach, M. Häberlen, J. K. N. Lindner, B. Stritzker, Nucl. Instr. Meth. B 242 (2006) 679.

[15] D. Chen, Z. M. Liao, L. Wang, H. Z. Wang, F. Zhao, W. Y. Cheung, S. P. Wong, Opt. Mater. 23 (2003) 65.

Figure Captions

(1) Cross-sectional transmission electron microscopy (XTEM) image of a $Si(100)$ sample implanted with $180\,keV\ C^+$ ions at a fluence of $4.3 \times 10^{17}\,cm^{-2}$ and a substrate temperature of 150 °C. Lamellar and spherical amorphous inclusions at the interface of the continuous amorphous layer are marked by L and S.

(2) Schematic explaining the selforganised evolution of amorphous SiC_x precipitates into ordered SiC_x lamellae with increasing fluence (see text).

(3) Comparison of simulation and XTEM ($180\,keV\ C^+$ implantation into silicon at 150 °C) for several fluences. Amorphous cells are white. Simulation parameters: $p_b = 0.01$, $p_c = 0.001 \times (3\,nm)^3$, $p_s = 0.0001 \times (3\,nm)^5$, $d_r = 0.05$, $d_v = 1 \times 10^6$.

(4) Depth distribution of amorphous cells (white) (a) and corresponding carbon concentration profile for a fluence of $4.3 \times 10^{17}\,cm^{-2}$ (b) that shows separately the mean amount of carbon in amorphous and crystalline volumes as well as the sum of both.

(5) Prediction of the selforganised formation of amorphous nanolamellae upon $2\,MeV\ C^+$ irradiation of silicon homogeneously doped within the top $500\,nm$ with $10\,at.\%$ carbon. The fluence increases from (a) to (f) with 100×10^6 simulation steps corresponding to a fluence of $2.7 \times 10^{17}\,cm^{-2}$.

Figures

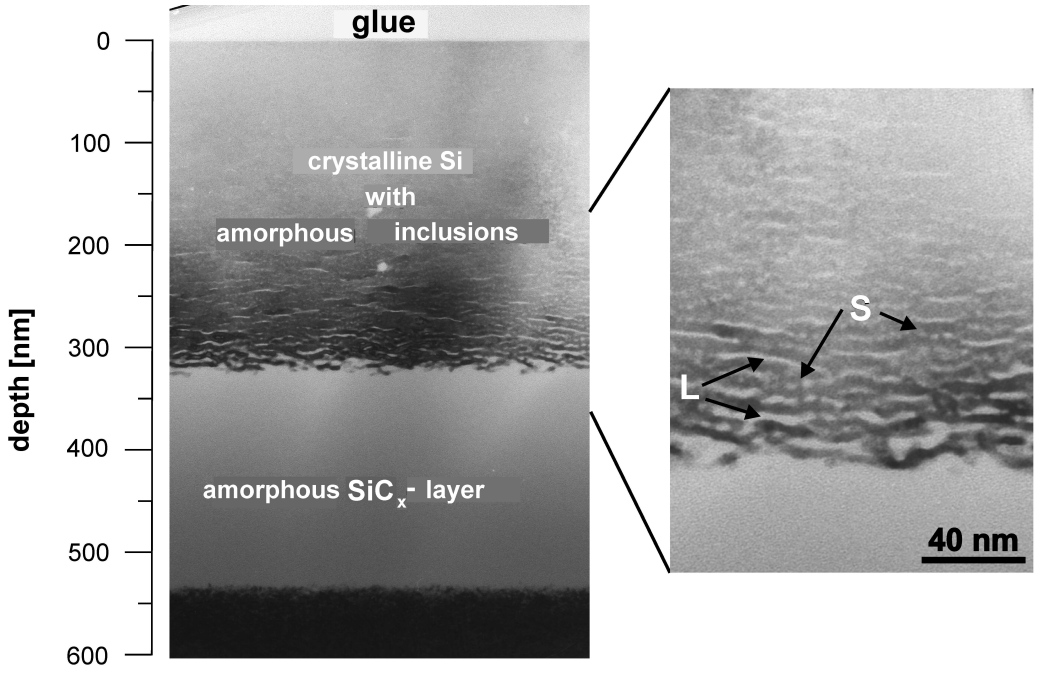

Figure 1.

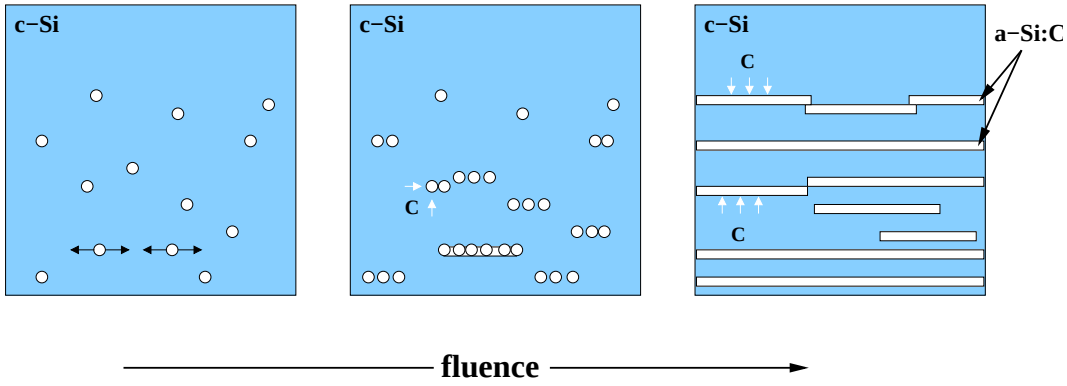

Figure 2.

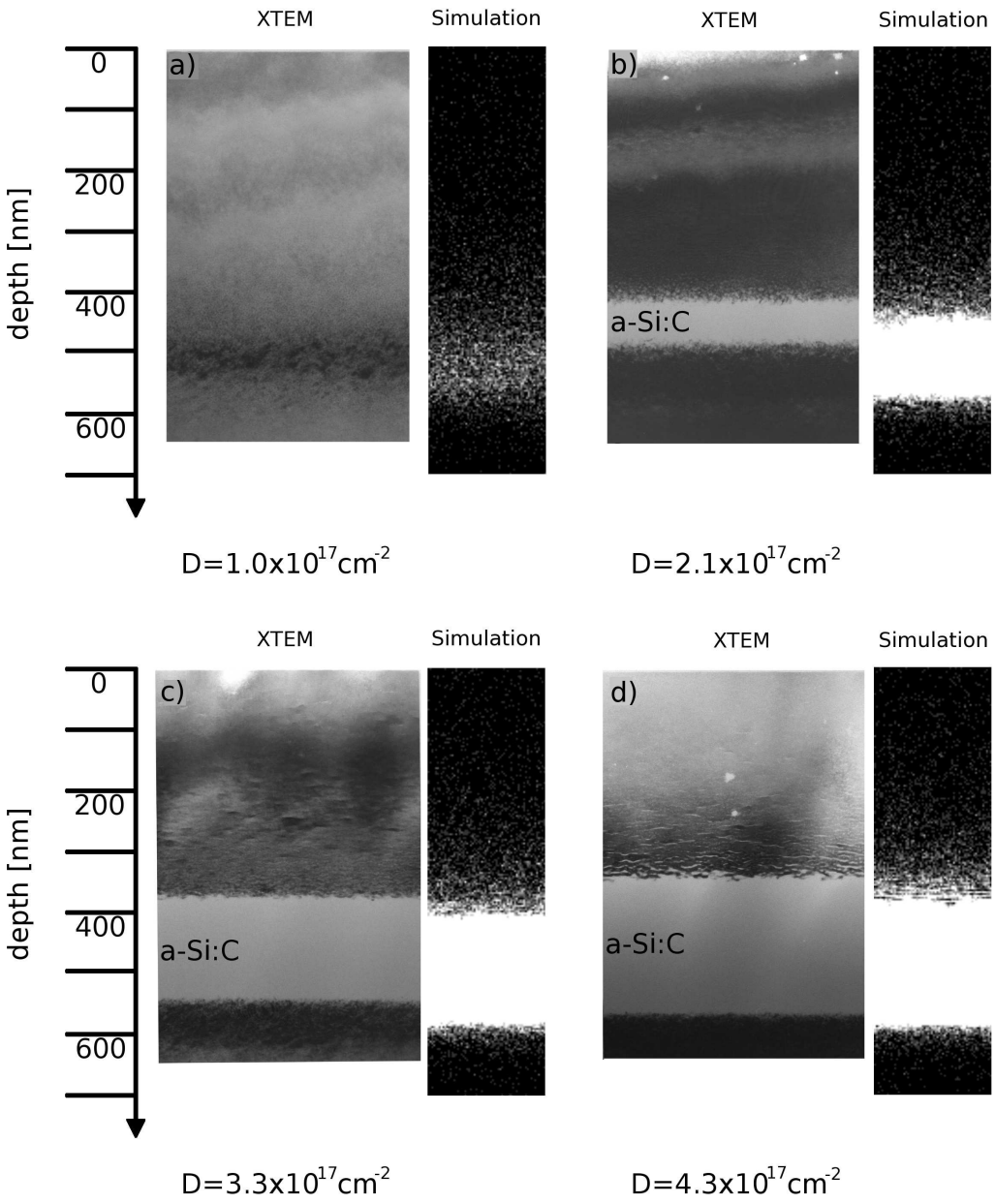
XTEM
Simulation
XTEM
Simulation
depth [nm]
0
200
400
600
a)
b)
a-Si:C
D=1.0x10^17cm^-2
D=2.1x10^17cm^-2
XTEM
Simulation
XTEM
Simulation
depth [nm]
0
200
400
600
c)
d)
a-Si:C
a-Si:C
D=3.3x10^17cm^-2
D=4.3x10^17cm^-2

Figure 3.

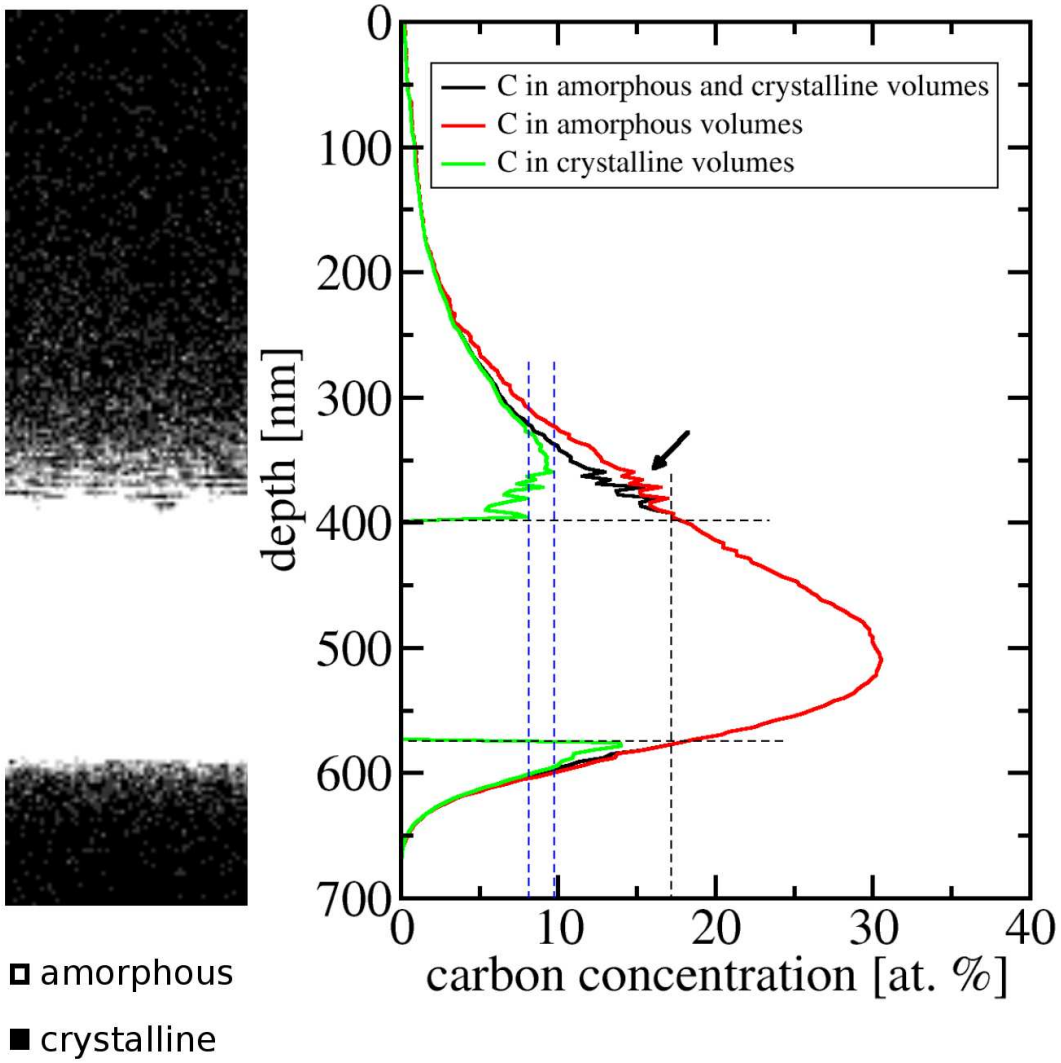
C in amorphous and crystalline volumes
C in amorphous volumes
C in crystalline volumes
depth [nm]
0
100
200
300
400
500
600
700
0
10
20
30
40
carbon concentration [at. %]
amorphous
crystalline

Figure 4.

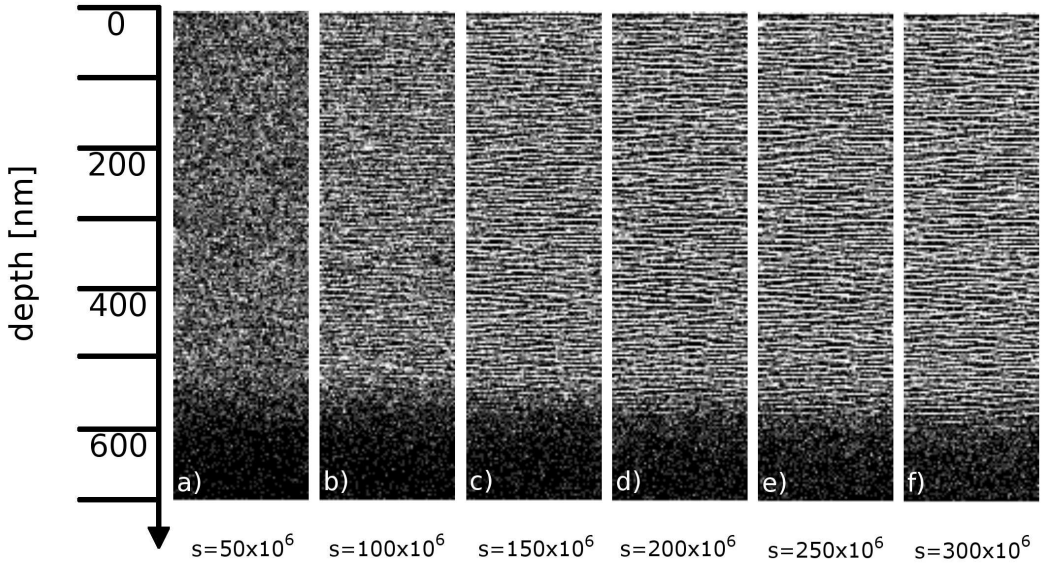
depth [nm]
0
200
400
600
a)
b)
c)
d)
e)
f)
s=50x10^6
s=100x10^6
s=150x10^6
s=200x10^6
s=250x10^6
s=300x10^6

Figure 5.